LA-UR -85-3620

CONF-851D160--12

MASTER

Los Alamos National Laboratory is operated by the University of California for the United States Department of Energy under contract W-7405-ENG-36

TITLE THE REPRESENTATION OF ORIENTATION DISTRIBUTIONS

LA-UR--85-3620

DE86 002419

AUTHOR(S) H. R. Wenk and U. F. Kocks

SUBMITTED TO To be presented at the symposium "Use of Crystallite Orientation Distribution Functions for Analysis of Texture and Prediction of Properties," ASM Fall Meeting, Toronto (Canada) 14 October 1985.

DISCLAIMER

Los Alamos Los Alamos National Laboratory
Los Alamos, New Mexico 87545

FORM NO. 836 R4
ST. NO. 2629 5/81

THE REPRESENTATION OF ORIENTATION DISTRIBUTIONS†

H. R. Wenk

Department of Geology and Geophysics

University of California, Berkeley, CA 94720

and

U. F. Kocks

Center for Materials Science

Los Alamos National Laboratory, Los Alamos, NM 37545

FINAL DRAFT 6 OCTOBER 1985

To be presented at the symposium "Use of Crystallite Orientation Distribution Functions for Analysis of Texture and Prediction of Properties", ASM Fall Meeting, Toronto (Canada), 14 October 1985.

---

† Work supported by the U.S. Department of Energy.

1. INTRODUCTION

It is widely acknowledged that texture is the prime cause of anisotropy in polycrystalline metals: the nonrandom distribution of the crystallographic orientations of the grains ('preferred orientation', 'texture', or 'fabric') transfers some of the anisotropic properties of single crystals to the aggregate. Whereas some properties show little or no anisotropy even in single crystals, many properties are strongly anisotropic even in materials with a cubic lattice.

A nonrandomness of the orientation distribution is virtually everpresent in metals, because all processes involved in producing such materials (casting, deformation, recrystallization) are locally orientation dependent. Texture studies are, in fact, frequently used by metallurgists to help identify the crystallographic details of such processes.

Despite this general recognition of the importance of texture for a description of macroscopic properties, it seems that quantitative evaluations of texture are rarely used in engineering practice or even in academic physical metallurgy, outside a small community of texture experts. In general applications, one or two pole figures are given at best, or some idealized orientations ('texture components'), with a qualitative interpretation of the expected effects. This is so even though sophisticated quantitative descriptions of three-dimensional orientation distributions have been available for twenty years [1-3].

Why has there been such inertia in using quantitative texture descriptions as a general tool of deformation studies? We submit that this is primarily due to some unfortunate choices that were made by the pioneers of this development, with respect to the graphic <u>representation</u> of orientation distributions. Of course, any representation may appear

easy once it has become familiar; but some provide a significant activation barrier upon first contact.

A number of alternative representations have been suggested in the literature but have, for some reason, not become common. We find a particular combination of these especially easy to visualize for the uninitiated, easy to assess qualitatively, and easy to evaluate quantitatively. These plots use polar rather than Cartesian coordinates (as proposed by Williams [3] and by Pospiech and Lucke [4,5]), and equal-area projections (as they are commonly used in geology [6]). We will describe these representations in the present paper, and also review in tutorial form some of the basic concepts of orientation distributions in uniform terminology.

In addition to graphic representations of orientation distributions, algebraic ones were introduced right at the beginning of this development; particularly, the definition of a continuous orientation distribution function (ODF), and its expansion in generalized spherical harmonics. This provides an elegant and concise description for some applications (such as tensor properties), but becomes cumbersome when very many terms are needed. In such cases, a useful graphic representation of the data is essential for a quantitative analysis.

A complete description of orientation distributions requires a three-dimensional orientation space. On the other hand, two-dimensional projections of this space is what is measured. There are various ways of inferring a 3-dimenional distribution from a number of 2-dimensional projections, and it has been a topic of intensive recent debate to what extent, under what circumstances, this can be done unambiguously [7-11].

This current interest provides a further reason for us to clarify the descriptions. For the purpose of this paper, we will assume that the three-dimensional orientation distribution is known, by theoretical prediction or by some deconvolution of experimental measurements; we only concern ourselves with the representation of a known distribution.

We will illustrate the principles presented with a particular experimental texture: from the surface layer of a copper polycrystal cold-rolled to 60% reduction in thickness. Four incomplete pole figures (200, 220, 222, and 113) were determined by x-ray diffraction in reflection geometry. The measured pole figures nearly exhibited orthorhombic symmetry (as expected), which was then strictly enforced by averaging the four quadrants of the pole figure. The orientation distribution function was obtained using the expansion in spherical harmonics (with only even-order coefficients up to $\ell = 18$). Inasmuch as this is only meant to serve as an example, neither the detailed sample history nor the pole figure deconvolution procedure are of essence.

2. DIRECTION SPACE AND ORIENTATION SPACE

While the description of (two-dimensional) directions is relatively trivial, we will review it in detail, because we find it important to preserve some continuity between the two- and three-dimensional cases -- more continuity than has generally been made use of.

In some cases, only the distribution of a single direction is of interest: e.g, the distribution of c-axes in a hexagonal material with respect to the normal of a sheet; or the distribution of the tensile axes in the stereographic triangle characterizing each grain of a cubic polycrystal. Such distributions are easy to treat quantitatively: the point

density on the surface of a unit sphere characterizes the distribution of directions in a uniform way. It may be represented by various projections, and it may be simplified by the application of symmetry principles--which we shall summarize in Section 3.

A particular symmetry deserves mention: namely when the sign of the direction is of no concern. Unsigned directions are often called 'poles' or 'axes'; we shall use pole for the unsigned normal to a crystallographic plane, as is common usage; and we shall use axis specifically for an unsigned sample coordinate. The distribution of either one with respect to some reference system can be described by point densities on the surface of a hemisphere. (Signed directions may be called 'unit vectors'; they are represented on the surface of a whole sphere.)

Whereas the term 'orientation' is sometimes loosely used in the same sense as 'direction' was used above (such as in 'the orientation of the tensile axis'), we wish to reserve the term orientation for the relation between an entire coordinate system (triad) and some reference triad. This requires the specification of three (perhaps perpendicular) axes or, more commonly, of two unit vectors and a handedness.

It took a long time for an appropriate description of orientation distributions to be developed [1,2]: i.e., an orientation space in which a uniform point density corresponds to a uniform (e.g. random) distribution of orientations, analogous to the surface of a sphere in the case of directions. We will call such spaces 'homochoric'. One easy solution is as follows (Fig. 1): describe the first direction (usually called Z or x_3 or [001]) just like any direction, and the second (perpendicular) direction (usually called X) by an azimuth around the first. A useful image is that of a boat at location Z on the surface of the earth, which

is heading in direction X. Specification of the first direction requires two numbers (the ship's longitude and latitude), that of the second direction requires one more number (the ship's heading, or azimuth). There is some arbitrariness in the precise specification of these three angles and their zeroes, but Euler angles are most commonly used and quite adequate. We shall apply the term Euler space to any three-dimensional space in which the coordinates are determined in some way by these three angles [5]; it is the precise structure of this space that we shall discuss, with the aim of making it homochoric.

There is an aesthetic flaw in this Euler space description of orientations: namely, that one direction (the 'first' direction used above) must be preferred by the observer, even if no such preference is inherent in the physics. For example, the roll' plane normal is commonly preferred over the rolling direction, although both have equivalent status. This artificiality can only be alleviated by preferring various poles or axes in succession, perhaps until one is found that is most easily visualized --or by showing two or three of these representations in parallel.

Two other descriptions of orientation relations are sometimes used, for specific reasons [5]. One is in terms of a particular axis in space (or a number of symmetrically equivalent ones) around which a single rotation brings the two triads into coincidence. This has been useful, e.g., in mechanistic discussions of recrystallization [12]; it is quite different from the description we use (in terms of a direction in one of the coordinate systems and an azimuth around it), which is completely equivalent to the three-rotations scheme of introducing Euler angles [13].

Finally, the orientation of one triad with respect to another can be described by a rotation matrix [5,14]. This description is easiest in

computer codes. It does not prefer any one axis; but the three numbers necessary for a complete specification do not form a homochoric space.

3. REPRESENTATION OF DIRECTIONS

3.1 Equal-area and stereographic projections

The location of a point on a sphere is easily described in the familiar geographic terminology of longitude and latitude. Following Bunge [13], we will use the longitude* β and the co-latitude α (also called pole distance).

A point on the sphere is then projected onto a plane by means of some standard projection. Stereographic and equal-area projections are most widely used. Projections always distort a true representation. In the stereographic projection (almost exclusively used in metallurgy) equal great-circle segments have the same length wherever they appear on the sphere. In equal-area projection (commonly used in geophysics) equal areas on the sphere have the same size in projection. This is best illustrated by projections of the coordinate system, which provides a Wulff net (Fig. 2a) and a Schmidt net (Fig. 2b) respectively. Either net is easily used for graphic constructions and the determination of angular relationships. While stereographic projection is most appropriate when the angles between crystal directions are of prime concern, equal-area projection would seem more appropriate when population densities are to be described. (An advantage of the stereographic projection is that circles remain circles--but their centers do not remain their centers.)

---

* β is also sometimes called an azimuth, but we reserve this term for the "heading" introduced above; see also sec. 4.1.

Figure 3 shows a {100} pole figure of a typical copper texture, both in stereographic (Fig. 3a) and equal-area projection (Fig. 3b). Pole densities are experimentally averaged into a continuous distribution and contours are expressed in multiples of a random distribution ("m.r.d."). Note that the (100) pole figure of a cubic material displays all three {100} orientations for each grain--but it does not give direct information on which {100} is in fact the specific (001) pole for a specific (100), for one grain. It is for this reason that pole figures are usually insufficient for a quantitative description of textures; but they are the most quantitative experimental information available.

3.2 Pole figures and 'inverse pole figures'

In the last section, the sample axes were chosen as a reference system, and the crystallographic poles were described in this frame. A completely equivalent description is its inverse (or dual): that of sample axes in terms of crystal axes. Sometimes one is more appropriate, sometimes the other. For example, when the sample is a wire, there is no natural sample triad, and all pole figures degenerate into circles; but a description of the wire axis distribution in terms of the crystal axes -- an 'inverse pole figure'-- is illustrative. Conversely, when the most appropriate sample axes (e.g., the most symmetric ones) are not known sufficiently accurately beforehand, a pole figure provides information on the actual sample symmetry, and thus guidance in selecting 'sample' axes.

For cubic materials, which we emphasize in the present paper, the three <100> directions provide a ready reference frame for inverse pole figures. Cubic symmetry reduces the area on the sphere that is necessary for a complete description by a factor 24: only 2 of the 48 unit triangles are needed, even if the plotted axis has no symmetry; if it lies in a mirror plane of the sample, a single triangle suffices [15].

Figure 4a shows one quadrant of the unit hemisphere, as it is usually projected: with the preferred pole (001) at the center. This makes the center a special point. One effect is that the mesh units have very small area there; if the constant-Φ lines were drawn such as to make each mesh unit encompass equal area, the units near the center would attain a very anisotropic shape. The unit triangles under cubic symmetry are also shown: any one of the three triangle-pairs (labelled I, IIa/b, and III) suffices for the most general case; but the special nature of the origin would seem to make pair I an especially poor choice.

Figure 4b shows a different scheme: the preferred pole (001) has been moved to the periphery [3]. In this case, it is possible to have similar and equi-axed unit areas everywhere. (Fig. 4b is an equal-area projection, see Fig. 2b.) The preferred triangles are shown in what appears to us to be the most convenient way (and rather conventional). For a numerical description, it would seem easier to use the latitude λ (rather than the co-latitude α'), and a longitude μ (for meridian) counted from (100).

Figure 5 demonstrates the case of the particular copper sample whose measured pole figure was shown in Fig. 3. Use is now made of the expected orthorhombic symmetry of the rolled sample (which was essentially verified in Fig. 3), to plot only one quadrant of the {100} pole figure. Also, this is complemented by a {111} pole figure (also measured and folded into one quadrant). Finally, two inverse pole figures, for the X^S and Z^S axes (rolling direction RD and rolling plane normal ND, respectively), were derived from these pole figures and are plotted in Fig. 5.

4. REPRESENTATION OF ORIENTATIONS

4.1 Previous representations

In the last figure (Fig. 5c, d), we showed in parallel two inverse pole figures, one for X^S = RD and one for Z^S = ND. This gives almost all information about the three-dimensional relation between the axis system X^S, Y^S, Z^S and the crystallographic reference system X^C = <100>, Y^C = <010>, Z^C = <001>, and such two figures together are in fact often sufficient to characterize an orientation distribution. What is missing is information on the correlation between the X^S-axis of each particular grain and its Z^S-axis.

It is for this reason that a truly three-dimensional representation is necessary in general. One easy way to introduce it is to plot, for example, an inverse pole figure for Z^S and perpendicular to it the amount of rotation around this preferred direction [3,4]. Another good method is to attach ticks to the points in an inverse pole figure to indicate the rotation around this point [16] much like in the "boats on the earth" picture introduced above; the disadvantage of the latter is that it works only for discrete points, not for continuous distributions. Neither of these procedures is easily applicable to pole figures, if there is more than one equivalent pole. Nevertheless, the basic idea, we feel, is of compelling simplicity: to represent an orientation by one direction (that of the arbitrarily preferred axis) and a rotation around it; this (last) rotation we shall call an azimuth (and count it from the equator). This description makes open use of the need to prefer one direction; and it retains continuity with the description of directions when only directions are important. We shall elaborate on two specific representations based on this principle below.

In texture research, another description, introduced by Bunge [1] and Roe [2], has become common, which is entirely equivalent, only differently phrased and differently represented. Here, three successive rotations are performed around the coordinate axes of the reference system (in a certain sequence), by the three Euler angles ϕ_1, Φ, ϕ_2 (Fig. 6).* In the sample reference frame, the first two rotations are exactly equivalent to the angles β and α used before: they do describe a direction, and ϕ_2 measures an azimuth around this direction --just as in the description used above. However, $\{\phi_1,\Phi,\phi_2\}$ are usually treated as three parameters on equal footing, and plotted in a three-dimensional space. The problem is that this space was chosen to be Cartesian [17]. This is equivalent to projecting the hemisphere on which the directions (ϕ_1,Φ) are uniformly distributed onto a square: the entire advantage of using a homochoric space (the Euler space) has been lost in its representation. An advantage is that the periodicity in all three rotations can be seen: the Cartesian Euler space can in fact be represented by a space lattice with orthorhombic symmetry (but no inversion center)[18,19].

The graphic representation of orientation distributions in this Cartesian space of Euler angles can be shown by contour lines in a series of two-dimenional sections, and this diagram has become so common as to be virtually identified with the abbreviation ODF. Figure 7 shows such a plot, for the same copper sample illustrated before. Note that the representation is severely distorted: the single orientation, in each section,

* We are staying as close as possible to Bunge's conventions [13]. Most type fonts contain only the straight or only the curly version of lowercase phi: they should be treated as completely equivalent. All three rotations increase counterclockwise (looking down on the positive axis) in the sample frame, clockwise in the crystal frame. In the sample frame, ϕ_1 measures the angle from $-Y^S$ to $+Z^C$, ϕ_2 from the equator to $+X^C$. In the crystal frame, ϕ_2 counts from $+Y^C$ to $+Z^S$ and ϕ_1 from the equator to $+X^S$. (The asymmetry in these relations stems from keeping $\Phi \geq 0$.)

for which $\Phi = 0$ is represented by a line.

In the inverse description, an orientation may be specified as that of the sample triad in the reference frame of the crystal. The preferred direction is usually taken to be Z^S; $\{\phi_2,\Phi\}$ become its longitude and latitude, respectively, and ϕ_1 the azimuthal rotation around Z^S. (For the convential signs, see the last footnote.) Figure 8 sketches one constant ϕ_1-section. This figure is the exact analog to Fig. 4a: it is evident how the singular point in Fig. 4a has been stretched out into the line $\Phi = 0$ in Fig. 8. It is also clear that a symmetry reduction to region I is an especially unfortunate choice. Region III, on the other hand, is close to the familiar description in terms of triangles.

4.2 Polar coordinates: the COD

Most of the difficulties of visualization disappear when the angle pair $\{\phi_1,\Phi\}$ is represented in polar coordinates, just as in a pole figure; the third angle, ϕ_2, can then be represented in a third dimension, perpendicular to the polar plot [5,20]. We call this a COD (crystal orientation distribution). For a two-dimensional image, a set of sections through this space at constant values of ϕ_2, with contour lines, is adequate.

A ϕ_2-section of the COD may be viewed as a "partial" {001} pole figure which shows the distribution of only those (001) poles that have corresponding (100) poles rotated ϕ_2 degrees away from the equator. Figure 9 displays a set of such partial pole figures for the copper specimen. These ϕ_2-sections of the COD contain the same information as those in Fig. 7, but they are represented in polar rather than Cartesian coordinates, and in equal-area projection. It appears to us that such a polar representation of the COD is considerably easier to read than the traditional Cartesian way, which represents the ODF as a density function with three equivalent rotations. Let us list some of these advantages.

a) Orientations can be readily identified

Firstly, this is trivially true for directions, i.e. when only one axis is of importance: this is the advantage of having chosen a description in which first axis is explicitly given in the classical way. More generally, consider the maximum labelled C at $\phi_1 = 40°$, $\Phi = 66°$ in the $\phi_2 = 25°$ section. It contains (001) axes of those grains whose (100) axes lie 25° away from the equator. By means of an equal-area net we can construct the full crystal orientation (Fig. 10a). We see that (121) coincides with ND and $[1\bar{1}1]$ with RD; this is the well-known "copper" texture component [5]. For another case, consider the maximum labelled B at $\phi_1 = 35°$, $\Phi = 45°$ in the $\phi_2 = 0$ section. The analysis in Fig. 10b shows that this orientation has (011) parallel to ND and $[2\bar{1}1]$ parallel to RD: the "brass" texture component.

b) Angles can be directly measured in the diagram

Assume we would like to know the relation between the two orientations that are associated with the C and B maxima discussed above, expressed as a rotation about a single axis. This is demonstrated in Fig. 10c: construct the two orientations as in (a), superpose the two diagrams, and find the two bisectors (dotted): their intersection marks the axis of rotation (<210>), and the angle ω (= 35°) of the rotation around this axis that brings the two orientations into coincidence is easily read off. (This is not a unique solution because of the high crystal symmetry [12]).

c) The symmetry is clearly displayed

Crystal and sample symmetry cause certain orientations in the COD to be equivalent. For example, a four-fold symmetry axis in [001] causes ϕ_2 to repeat every 90°, and there is no need to extend ϕ_2-sections through a

full 360° span. In order to be complete, the sector shown in the COD must contain at least one orientation of each symmetrically equivalent set. A summary of equivalent orientations for important crystal and sample symmetries is shown in Table 1. In the case of cubic crystal symmetry and orthorhombic specimen symmetry, a range of ϕ_1 from 0° to 180°, of Φ from 0° to 90°, and of ϕ_2 from 0° to 45° is sufficient. A unit with all three angles going from 0° to 90° would also suffice, resulting in smaller sectors but more sections, which is less convenient for printing and also makes it more awkward to visualize angular relations. Both of these schemes still contain three equivalent orientations due to the three-fold axis along <111>; these are not easily recognized in the COD. Sometimes it is useful to choose to plot more than one irreducible unit to illustrate symmetry relationships.

Polar COD's are particularly useful to check how closely an assumed specimen symmetry is approached. For example, in our rolled copper specimens, the first-measured pole figures, based on the "given" coordinate axes ND and RD were clearly <u>not</u> close enough to orthorhombic symmetry. We redefined the sample axes until the pole figure exhibited satisfactory orthorhombic symmetry, and only then averaged the four quadrants as described above. Often it would be preferable to manipulate actual measurements as little as possible and to compare these "raw data" with theoretical predictions. In this case, variations that are smaller than the observed deviations from the appropriate sample symmetry should be treated as meaningless.

d) <u>There is a visible connection to the pole figure</u>

Viewing the COD as a set of partial {001} pole figures, with each ϕ_2-section containing the subset of (001) poles for a certain (100)

elevation, implies that the average of all ϕ_2-sections constitutes the complete {001} pole figure. This is the same as a projection along ϕ_2; it is shown in the last diagram of Fig. 9 and compares favorably with the measured (002) pole figure (Fig. 3b).

e) The representation is uniform

The space selected for representation and for projection (Euler space in polar equal-area projection) is homochoric with orientation space: equal densities seen are equal densities present. For this reason, we recommend equal-area projection also for pole figures [21]: it provides a better representation of the total fraction of crystals that contribute to a maximum (see Fig. 3a vs Fig. 3b).

The points (a) through (d) made above illustrate that a COD in polar coordinates is indeed easy to visualize and to analyze quantitatively. It displays all the information needed to derive full orientation relations using simple geometric constructions. If, in addition, one chooses equal-area plots, the visual impression is representative of the actual distribution (point e). The concept of viewing the COD as a pole figure deconvoluted into partial pole figures in orientation space is close in philosophy to the vector method [22].

4.3 The sample orientation distribution (SOD)

A description of sample axes in terms of crystallographic axes can make use of the same Euler angles. Now the pair $\{\phi_2,\Phi\}$ describes the direction (typically of the Z^S-axis) in the crystal system, just like in any inverse pole figure, and ϕ_1 describes the azimuthal rotation around this direction. An appropriate space for the SOD is thus an equal-area projection (or the part of it that is necessary according to the symmetry of the crystal, as in Fig. 4b) and a perpendicular dimension along which

ϕ_1 is plotted. It is seen that ϕ_1 and ϕ_2 have switched their roles as azimuth and longitude. Again, we can represent the three-dimensional SOD by a series of sections, this time at constant ϕ_1 (Fig. 11). A projection along ϕ_1 gives a Z^S-axis figure: an 'inverse pole figure'. In analogy to the term 'partial pole figure' which we tentatively introduced above for a ϕ_2-section, we may call ϕ_1-sections 'partial inverse pole figures'.

A similar concept was introduced by Williams in 1968 [3]: he represented three-dimensional orientation distributions by a series of partial inverse pole figures (which he called "axial pole figures"), and also showed how these can be derived from pole figures by the "matrix method" (quite similar to the "vector method" [22]). Williams used a definition for the azimuthal angle (his β) that differs from the Euler angle ϕ_1; while this has some advantages [3], it has the disadvantage that the duality between ϕ_1 and ϕ_2, i.e. between the SOD and the COD, gets lost. More significantly, using β as the third dimension in the SOD would not make a homochoric space. We therefore do not follow Williams in this respect.

In Fig. 11, each ϕ_1-section displays the distribution of those specimen normals Z^S = ND which have their X^S = RD axis ϕ_1 degrees off the equator (clockwise rotation, cf. Fig. 6b). As explained in detail before, a range of 0° to 90° in each of the three angles would be sufficient; in fact, there are still three equivalent orientations due to the three-fold <111>-axis. They are not easily recognized in the SOD sections (although they are evident in the projection). For example, the maxima at $\{\phi_1,\Phi,\phi_2\}$ = {0,45°,0}, {0,45°,90°}, and {90°,90°,45°} are equivalent. (For an analytical expression of this symmetry relation, see e.g. [19].) Because of this, only one unit triangle in Fig. 11 needs to be represented (an example is shown emphasized); but again, a larger

sector is often easier to visualize. In Fig. 11, we have chosen to show twice the necessary range in ϕ_2 (but it is not possible to compensate for this by reducing the range of ϕ_1 to be from 0° to 45°, as it could be done for ϕ_2 in Fig. 9).

A special point must be made regarding the center of the polar plots: the singular point where Z^S and Z^C are parallel, the 'North pole'. Here, the meridian is multivalued (ϕ_1 in the COD, ϕ_2 in the SOD). This corresponds to the physical situation (and was one of the reasons for us to abandon the Cartesian plots of Euler space). However, the heading of the boat is defined; thus, ϕ_2 has a meaning in the COD, ϕ_1 in the SOD. The trouble is that each is measured along the azimuthal great circle (the horizon) 'from the equator'; but in the special case $\Phi = 0$, the horizon and the equator are the same thing, and thus the value of the azimuth is undefined. It is easy to overcome this apparent difficulty, when it is realized that ϕ_1 and ϕ_2 are completely equivalent rotations in this case; in fact, the sum $\phi_1+\phi_2$ is the quantity that retains its meaning at the singular point. Thus, when we plot sections at constant azimuth, the value of the azimuth at the center point is meant to be that corresponding to the zero meridian.

Finally, we must emphasize that we have actually stayed with the conventional and expediant type of polar plot: with the singular point at the center--not, as suggested in Fig. 4(b), at the periphery. For cubic materials, the partial inverse pole figures (Fig. 11) could be converted by merely superimposing on them a net of the kind used in Fig. 4(b); one would then be able to choose a reduced region with minimal distortion. For the partial pole figures, one would have to write a new plotting routine, which would then be incompatible with conventional pole plots.

5. CONCLUSIONS

In the following, we summarize the points made in the present paper.

1) We have emphasized the distinction between directions (2-D quantities) and (3-D) orientations, but kept some continuity in their respective quantative descriptions.

2) We have re-emphasized the need for representations of direction space and orientation space that do not distort densities (and labelled such spaces 'homochoric'). The surface of a unit sphere is a homochoric direction space, Euler space is a homochoric orientation space. Unfortunately, it requires the preference, in the description, of one of the three coordinate axes defining an orientation--or, equivalently, of one direction (around which a rotation defines the third parameter). The preferred direction should be described like any direction: as a point on the surface of a unit sphere (e.g., by its longitude and co-latitude).

3) Two-dimensional representations of either the surface of a sphere or of a three-dimensional orientation space should preserve the homochoricity so strenuously achieved. Thus, the surface of a sphere should be projected in <u>equal-area projection</u>, which is just as easy to use as the stereographic projection, but much easier to visualize in terms of relative densities of directions. Similarly, three-dimensional orientation space should first be projected onto the surface of a sphere (to describe the preferred direction, e.g. in terms of its longitude and co-latitude); then, this surface should be projected onto a circle in equal-area projection; and finally, the third dimension may be represented by means of constant-azimuth sections. We find the analog of the positions and headings of boats on the surface of the earth helpful.

4) In application of these principles, we propose to use two dual orientation distribution representations: the COD, which represents the orientation of a crystal coordinate system with respect to a sample frame in terms of a set of partial pole figures (each containing those of the preferred poles that have a particular azimuth ϕ_2); and the SOD, which conversely displays the orientations of sample coordinate axes with respect to a crystal frame in terms of a set of partial inverse pole figures (each containing those preferred axes that have a particular azimuth ϕ_1). The final figure represented in each COD is the average partial pole figure (or ϕ_2-projection), which is a pole figure; similarly, the final figure shown in a SOD is the average partial inverse pole figure (or ϕ_1-projection): it is an 'inverse pole figure'. A summary of these conventions is given in Table 2. We find these polar representations of the orientation distribution much easier to visualize and evaluate than the Cartesian ODF representations that have become common.

5) The net to be used in any of the representations should, while consisting of constant-area units, be also equiaxed (rather than having very anisotropic shapes). This is possible when the least symmetric unit needed is chosen so as not to include the (North) 'pole' of the representation (see Fig. 4b).

Our principal concern has been to find two-dimensional graphic representations of three-dimensional orientation distributions that allow one to "see" something (with minimal distortion). We "like" two sets of circular sections; each set may be stacked up as a cylinder. Unfortunately, it is difficult to visualize a three-dimensional space through which the CODR and the SODR are different sections. This was easy in the conventional Cartesian Euler space.

In all of our discussion, we have assumed that the three-dimensional orientation distributions are known. To illustrate the proposed representations of orientation distributions, we have used a sample of a cubic metal deformed in rolling (and an oversimplified pole figure deconvolution). The same concepts have been applied to cases of lower crystal and sample symmetries, where the advantages are even more striking [23].

We end our discussion by outlining the specific, very minor changes that would have to be made in existing computer codes to implement our suggestions. The calculation of ODF's from pole figures is unaffected; but instead of using the contouring routine for a rectangular grid, one should use, for each ODF section, the pole-figure contouring routine (such as Vadon's URFPD). To convert from stereographic to equal-area projection, one simply must change the formula for the projection of the pole distance α from $\tan(\alpha/2)$ to $\sqrt{2}\cdot\sin(\alpha/2)$.

ACKNOWLEDGMENTS

The authors gratefully acknowledge many helpful discussions with K. Lücke, H. Mecking, and M. Hatherly, as well as instructive comments on the manuscript by J.S. Kallend, S. Matthies, and P.R. Morris; we also thank P.S. Follansbee for the Cu sample, and D. O'Brien and A. Vadon for permission to use their plotting programs. This work was supported by the U.S. Department of Energy, the IGPP of the University of California at Los Alamos, and the National Science Foundation.

REFERENCES

1. H.J. Bunge: Z. Metallk. 56, 872 (1965).

2. R.J. Roe: J. Appl. Phys. 36, 2024 (1965).

3. R.O. Williams: Trans. Met. Soc. AIME 242, 105 (1968); J. Appl. Phys. 39, 4329 (1968).

4. J. Pospiech and K. Lücke, Acta Metall. 23, 997 (1975).

5. J. Hansen, J. Pospiech, K. Lücke: "Tables for Texture Analysis of Cubic Crystals", Springer (1978).

6. H.R. Wenk: in "Preferred Orientation in Metals and Rocks", ed. H.R. Wenk (Academic Press, 1985) p. 13.

7. S. Matthies: phys. stat. sol. (b) 92, K135 (1979); Int. Conf. on Textures of Materials (Netherl. Soc. for Mater. Sci., Zwijndrecht, Netherlands, 1984) p. 737.

8. K. Lücke, J. Pospiech, K.H. Virnich, J. Jura: Acta Met. 29, 167 (1981)

9. H.J. Bunge, C. Esling, J. Muller: Acta Cryst. A37, 889 (1981).

10. J. Pospiech, Int. Conf. on Textures of Materials (Netherl. Soc. for Mater. Sci., Zwijndrecht, Netherlands, 1984) Supplement p. 13.

11. U.F. Kocks and H.R. Wenk: to be published.

12. G. Ibe, K. Lücke: Arch. Eisenhüttenwesen 39, 693 (1968).

13. H.J. Bunge: "Texture Analysis in Materials Science (Butterworths 1982)

14. R.J. Asaro and A. Needleman: Acta Metall. 33, 923 (1985).

15. P. van Houtte, E. Aernoudt: Mater. Sci. Eng. 23, 11 (1976).

16. P. van Houtte, E. Aernoudt: Z. Metallk. 66, 303 (1975).

17. P.R. Morris and A.J. Heckler: Adv. X-ray Analysis 11, 454 (1968).

18. D.W. Baker: Adv. X-ray Anal. 13, 435 (1970).

19. J. Pospiech, A. Gnatek, K. Fichtner: Crystal Res. Tech. 9, 729 (1974).

20. J. Pospiech: Crystal Research and Technology 7, 1057 (1972).

21. S. Gorczyca

22. D. Ruer, R. Baro: Adv. X-ray Anal. 20, 187 (1976).

23. H.R. Wenk: in "Preferred Orientations in Metals and Rocks", ed. H.R. Wenk (Academic Press, 1985) p. 370.

Table 1: Equivalent orientations for some crystal and sample symmetries

ϕ_1	Φ	ϕ_2	
$\phi_1 + \pi$	$-\Phi$	$\phi_2 + \pi$	identity
ϕ_1	Φ	$\phi_2 + \pi/3$	6-fold axis in Z^C (hexagonal)
ϕ_1	Φ	$\phi_2 + \pi/2$	4-fold axis in Z^C (cubic, tetrag.)
ϕ_1	Φ	$\phi_2 + 2\pi/3$	3-fold axis in Z^C (trigonal)
$\phi_1 + \pi$	$\pi-\Phi$	$-\phi_2$	2-fold axis Y^C
$-\phi_1$	$\pi-\Phi$	$\phi_2 + \pi$	2-fold axis in Y^S
$\phi_1 + \pi$	Φ	ϕ_2	2-fold axis in Z^S
$\pi-\phi_1$	$\pi-\Phi$	$\phi_2 + \pi$	2-fold axis in X^S

Table 2: Representations of the three-dimensional orientation distribution ODF(ϕ_1,Φ,ϕ_2)

2-D sections*	2-D projections
COD(ϕ_1,Φ); ϕ_2 = const "partial pole figures"	pole figure (β, α)
SOD(ϕ_2,Φ); ϕ_1 = const "partial inv. pole figures"	inverse pole figure (α',β')
*For Φ = 0, $\phi_1 + \phi_2$ = const	

CAPTIONS

Fig. 1 A direction Z is represented as a location on the surface of a sphere: by its longitude ϕ_1 and its pole distance Φ (perspective drawing). An orientation $g(\phi_1,\Phi,\phi_2)$ is represented by $Z(\phi_1,\Phi)$ and an azimuth ϕ_2 around it. An orientation distribution corresponds to a distribution of boats (with specified headings) on the surface of the earth.

Fig. 2 Projection of the coordinate grid on the sphere: (a) stereographic projection (Wulff net), (b) equal-area projection (Schmidt net).

Fig. 3 Experimentally determined {200} pole figure of copper rolled to 50% reduction at room temperature. Transverse (TD) and rolling (RD) direction are indicated. (a) stereographic projection, (b) equal area projection.

Fig. 4 (a) The quadrant of an inverse pole figure for cubic crystals as it is conventionally drawn. (b) An equivalent quadrant in equal-area projection, not including the special pole (001).

Fig. 5 {100} and {111} pole figures (a, b) and inverse pole figure for the ND and RD axis (c,d) for copper recalculated from the ODF with the harmonic analysis. Equal-area projection. Contour intervals are 0.5 m.r.d.; stippled below 0.5 m.r.d.

Fig. 6 Definition of Euler angles ϕ_1, Φ, ϕ_2 using the convention of Bunge [1], based on the sample coordinate system (a) and the crystal coordinate system (b).

Fig. 7 ODF of rolled copper, represented in conventional Cartesian coordinates. Contour intervals 0.5 m.r.d., stippled below 0.5 m.r.d. Constant-ϕ_2 sections, extending from 0° to 45°. The range of Φ is from 0 to 90° (down), that of ϕ_1 is from 0 to 180° (right).

Fig. 8 A section of conventional Cartesian Euler space (constant ϕ_1) for cubic materials with irreducible regions I, IIa/b, and III. Compare Fig. 4a. Region III is least distorted.

Fig. 9 COD of rolled copper represented as partial pole figures in equal-area projection, corresponding directly to Fig. 7. The last diagram is an average over all partial pole figures and corresponds to a (001) pole figure (Fig. 3 and Fig. 5a). The most common components of the f.c.c. rolling texture are indicated, by <u>one</u> representative: C - the 'copper' component $\{121\}\langle 1\bar{1}1\rangle$; S - the 'S' component $\{132\}\langle 6\bar{4}3\rangle$; B - the 'brass' component $\{011\}\langle 2\bar{1}1\rangle$; C - the 'Goss' component $\{011\}\langle 100\rangle$; and also the 'α-fibre'.

Fig. 10 Derivation of Orientation Relationships.
(a) Reconstruction of the crystal orientation for the maximum at $\phi_1 = 40°$, $\Phi = 66°$, $\phi_2 = 25°$ using the COD of Fig. 9 and an equal-area net (Cu component).
(b) Same as (a) for the orientation $\phi_1 = 35°$, $\phi = 45°$, $\phi_2 = 0°$ (B component).
(c) Superposition of (a) and (b) to determine the rotation axis and angle ω which brings the two orientations into coincidence.

Fig. 11 SOD of rolled copper represented as partial inverse pole figures. The test diagram is an average over partial inverse pole figures from $\phi_1 = 0°$ to $\phi_1 = 180°$ and corresponds to an inverse pole figure for the ND axis (Fig. 5c). The letters indicate f.c.c. rolling components as in Fig. 9, and the 'β-fibre'.

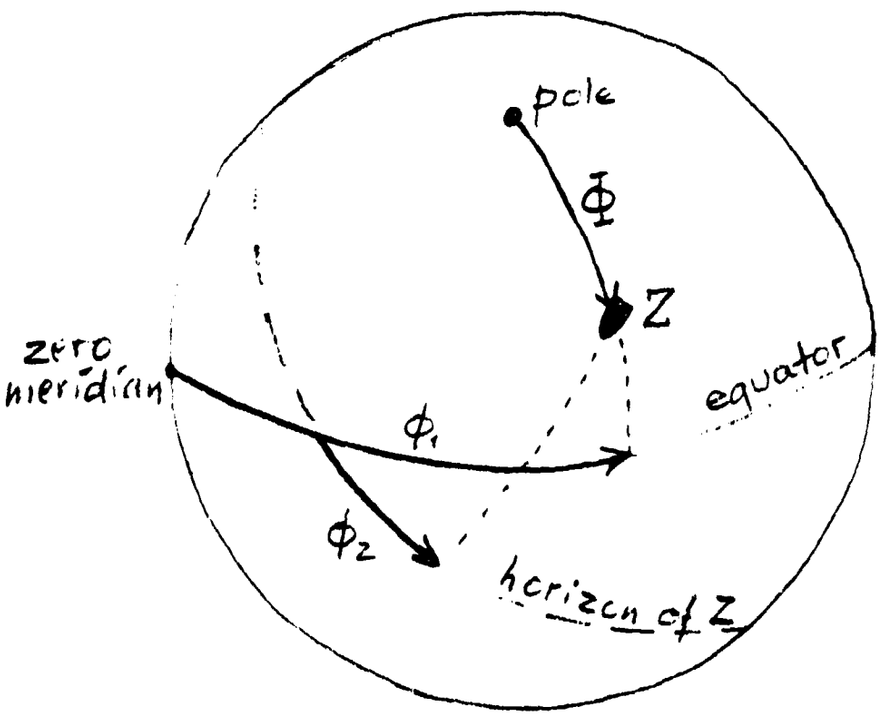

Fig. 1 A direction Z is represented as a location on the surface of a sphere: by its longitude ϕ_1 and its pole distance Φ (perspective drawing). An orientation $g(\phi_1,\Phi,\phi_2)$ is represented by $Z(\phi_1,\Phi)$ and an azimuth ϕ_2 around it. An orientation distribution correspouds to a distribution of boats (with specified headings) on the surface of the earth.

(a)

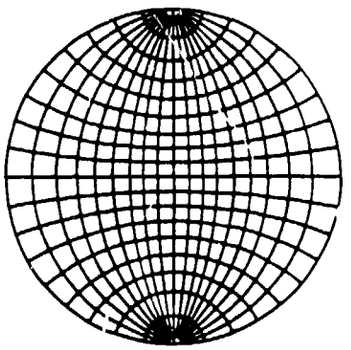

(b)

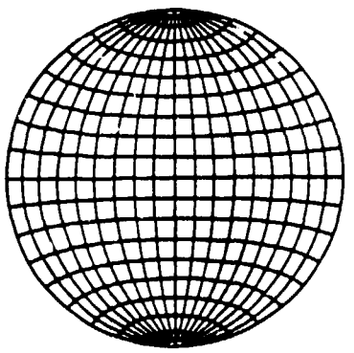

Fig. 2 Projection of the coordinate grid on the sphere: (a) stereographic projection (Wulff net), (b) equal-area projection (Schmidt net).

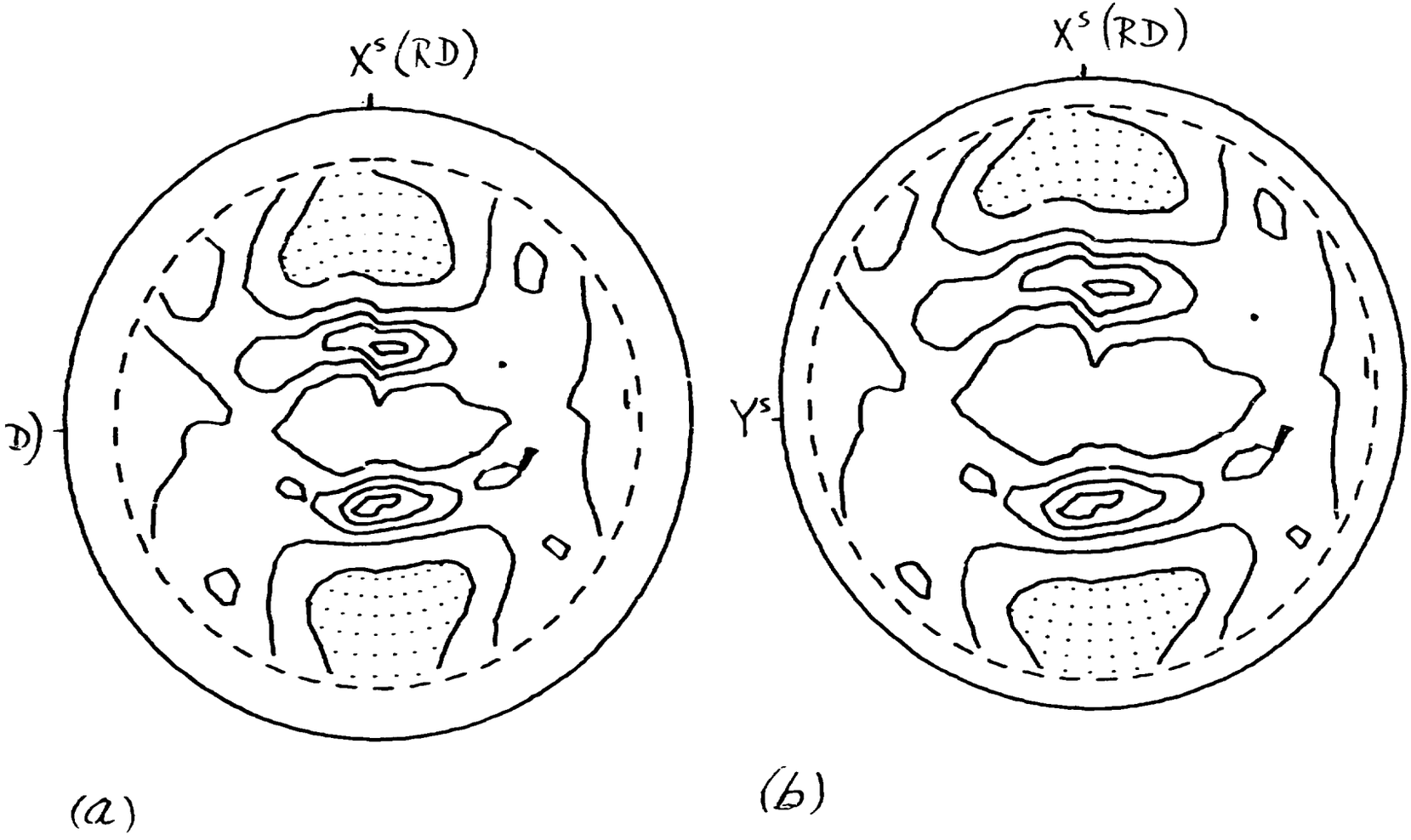

Fig. 3 Experimentally determined {200} pole figure of copper rolled to 50% reduction at room temperature. Transverse (TD) and rolling (RD) direction are indicated. (a) stereographic projection, (b) equal area projection.

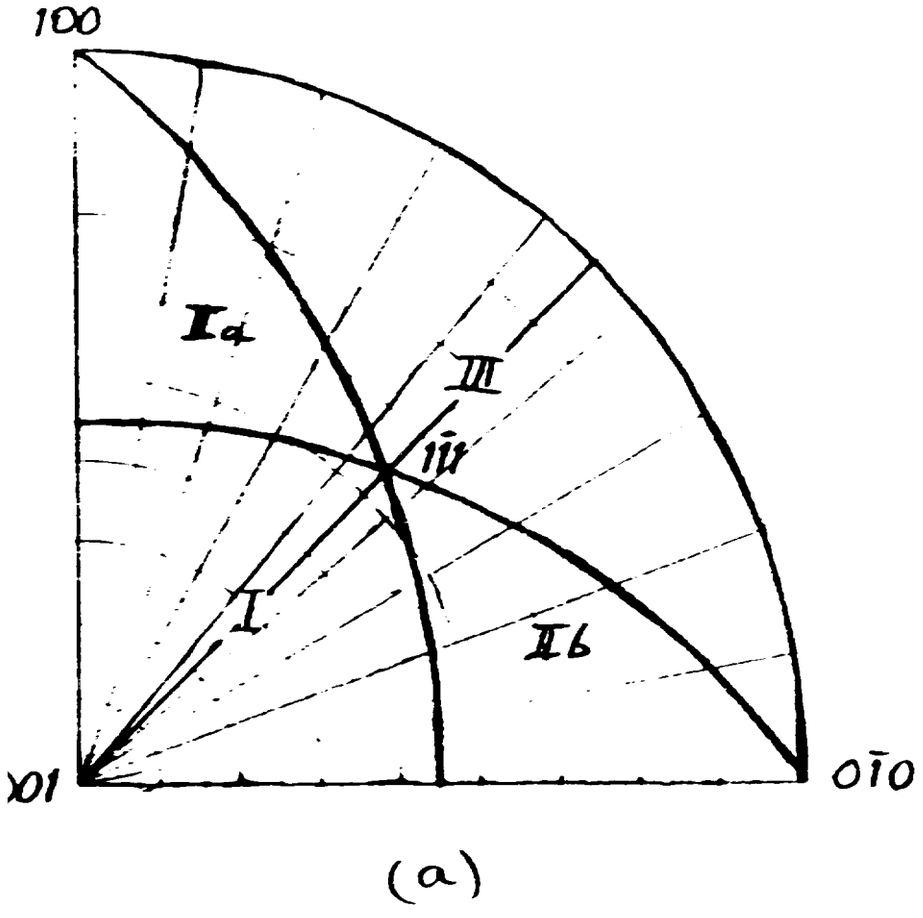

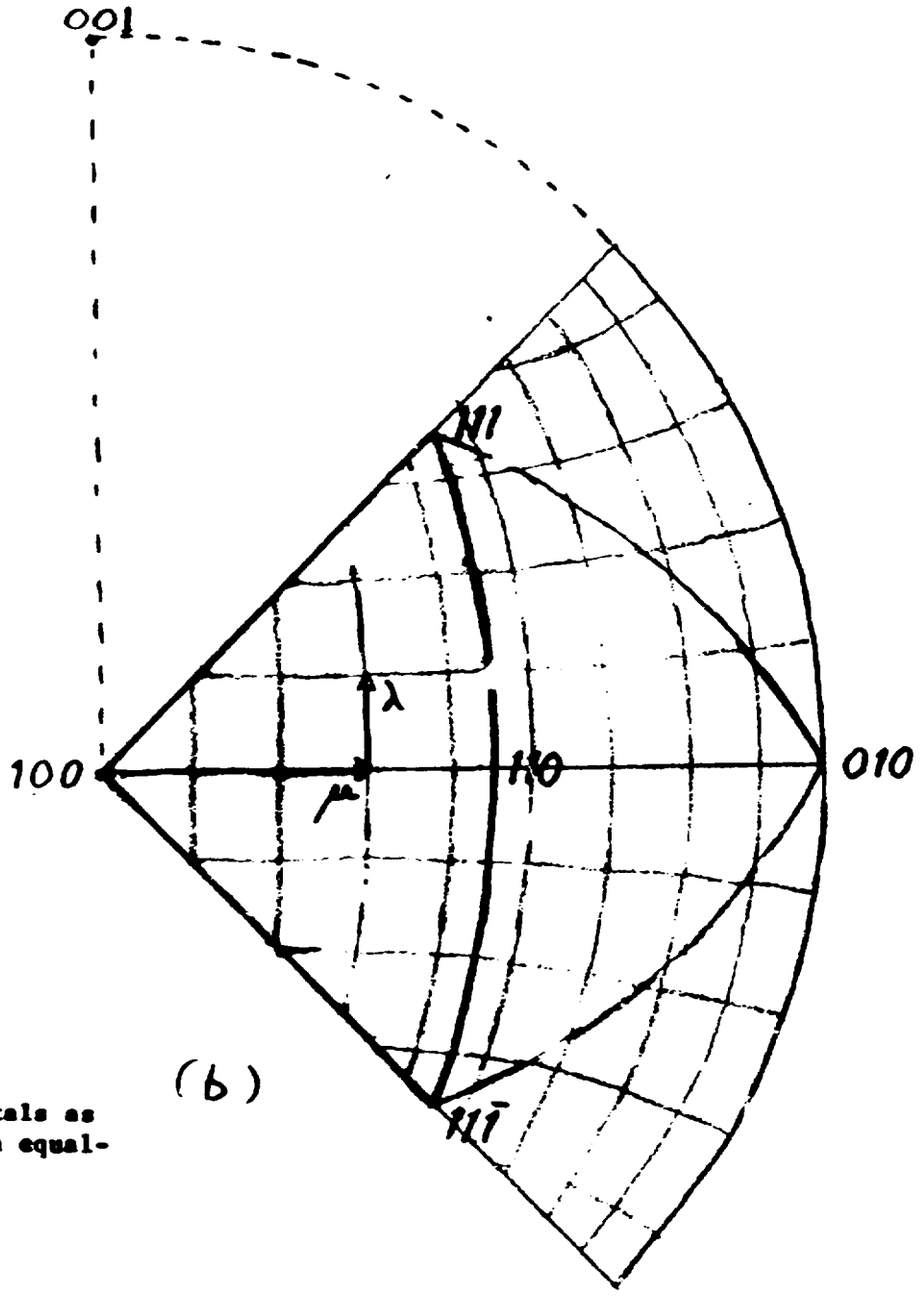

E. 4 (a) The quadrant of an inverse pole figure for cubic crystals as it is conventionally drawn. (b) An equivalent quadrant in equal-area projection, not including the special pole (001).

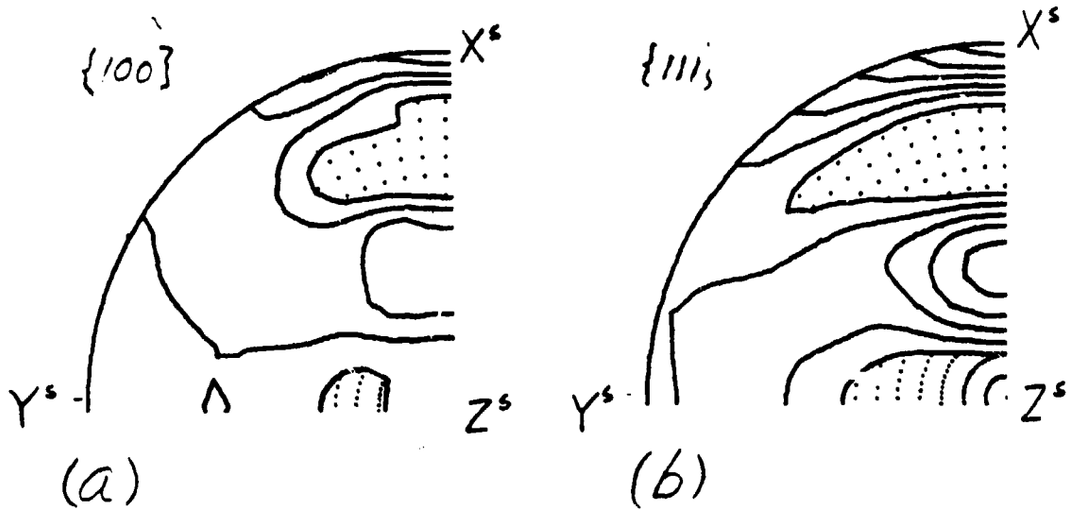

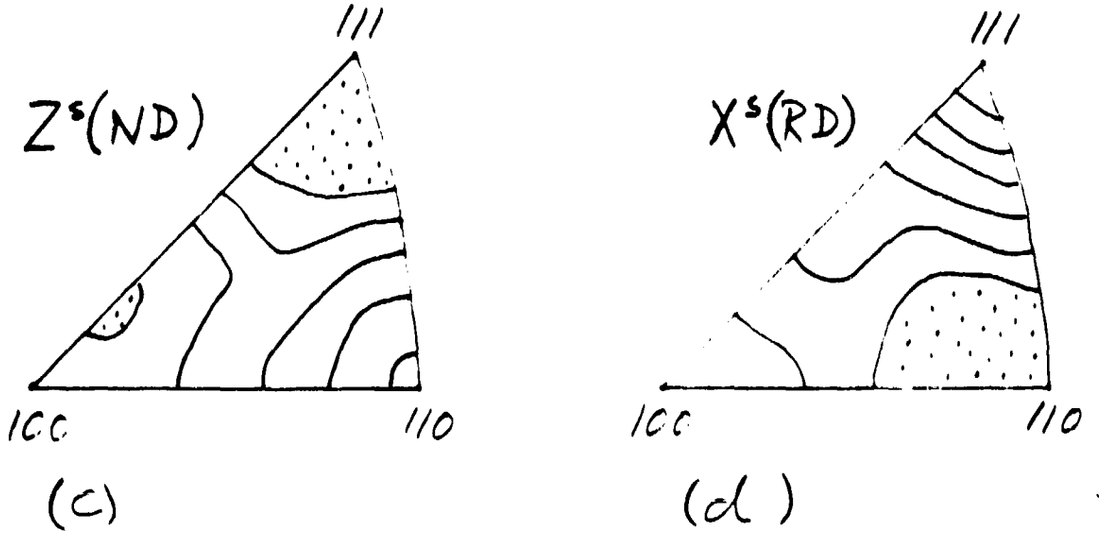

Fig. 5 {100} and {111} pole figures (a, b) and inverse pole figure for the ND and RD axis (c,d) for copper recalculated from the ODF with the harmonic analysis. Equal-area projection. Contour intervals are 0.5 m.r.d.; stippled below 0.5 m.r.d.

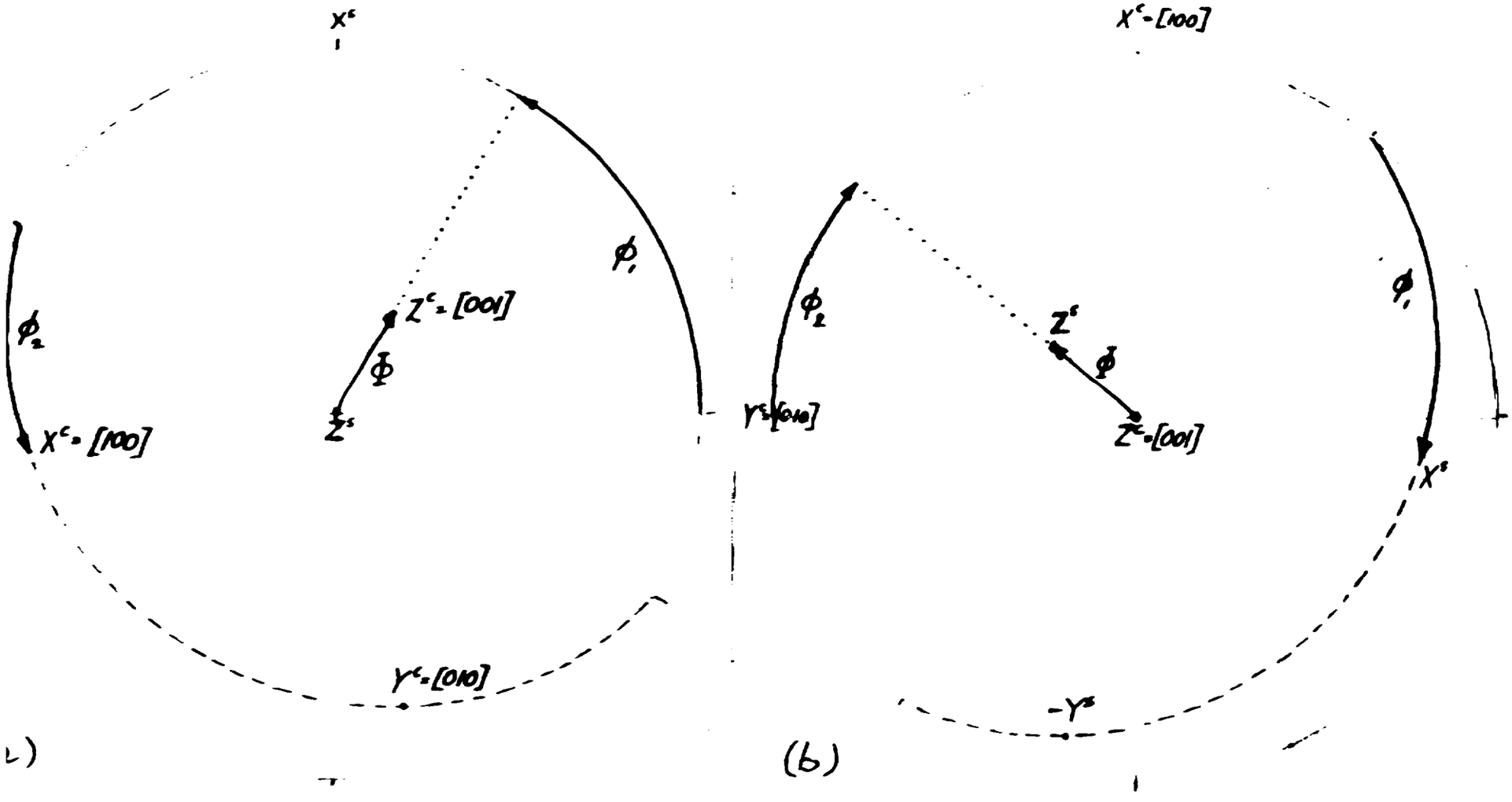

Fig. 6 Definition of Euler angles ϕ_1, Φ, ϕ_2 using the convention of Bunge [1] based on the sample coordinate system (a) and the crystal coordinate system (b).

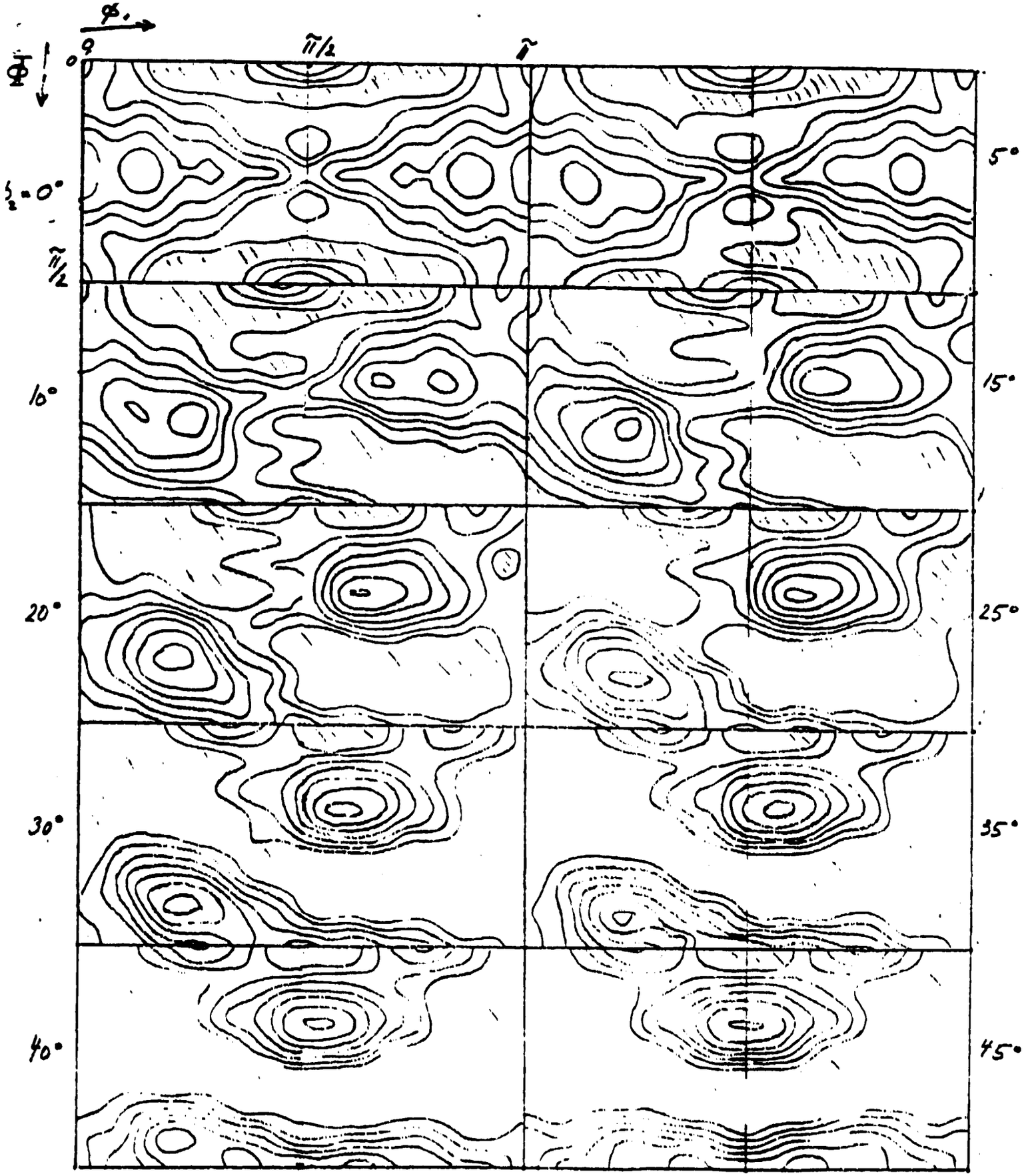

Fig. 7 ODF of rolled copper, represented in conventional Cartesian coordinates. Contour intervals 0.5 m.r.d., stippled below 0.5 m.r.d. Constant-ϕ_2 sections, extending from 0° to 45°. The range of Φ is from 0 to 90° (down), that of ϕ_1 is from 0 to 180° (right).

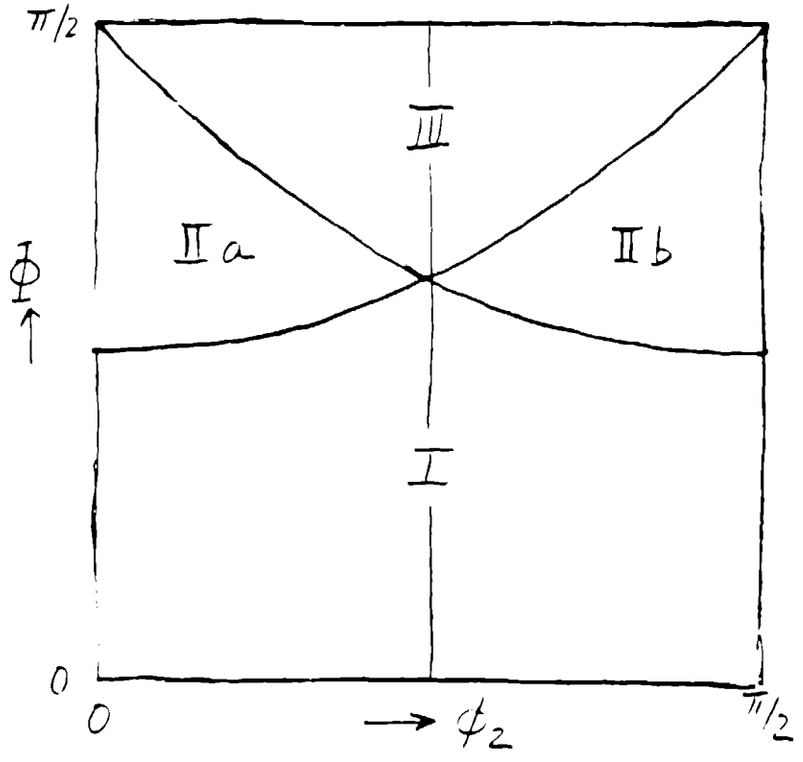

Fig. 8 A section of conventional Cartesian Euler space (constant ϕ_1) for cubic materials with irreducible regions I, IIa/b, and III. Compare Fig. 4a. Region III is least distorted.

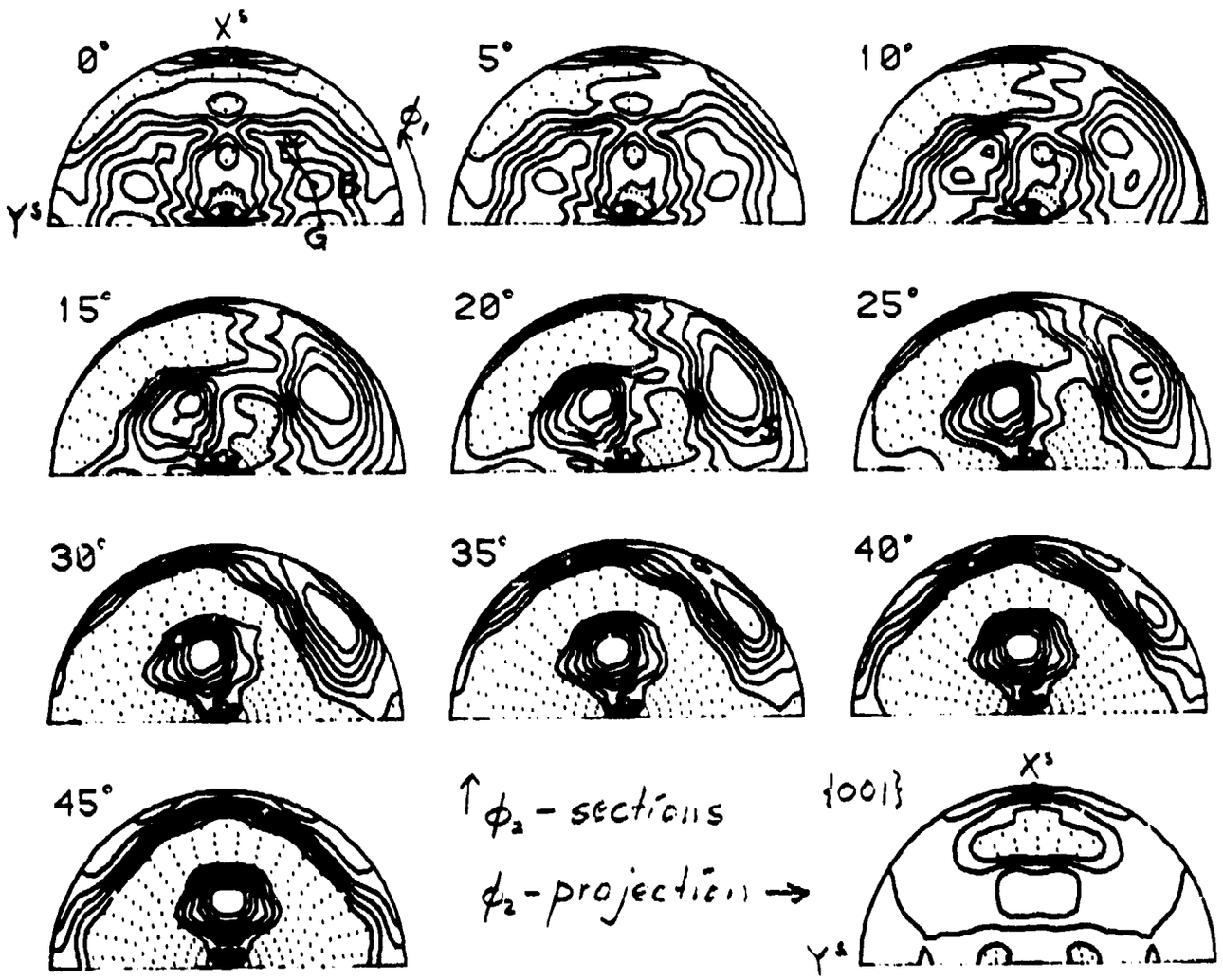

Fig. 9 COD of rolled copper represented as partial pole figures in equal-area projection, corresponding directly to Fig. 7. The last diagram is an average over all partial pole figures and corresponds to a (001) pole figure (Fig. 3 and Fig. 5a). The most common components of the f.c.c. rolling texture are indicated, by one representative: C - the 'copper' component $\{121\}\langle 1\bar{1}1\rangle$; S - the 'S' component $\{132\}\langle 6\bar{4}3\rangle$; L - the 'brass' component $\{011\}\langle 2\bar{1}1\rangle$; G - the 'Goss' component $\{011\}\langle 100\rangle$; and also the 'α-fibre'.

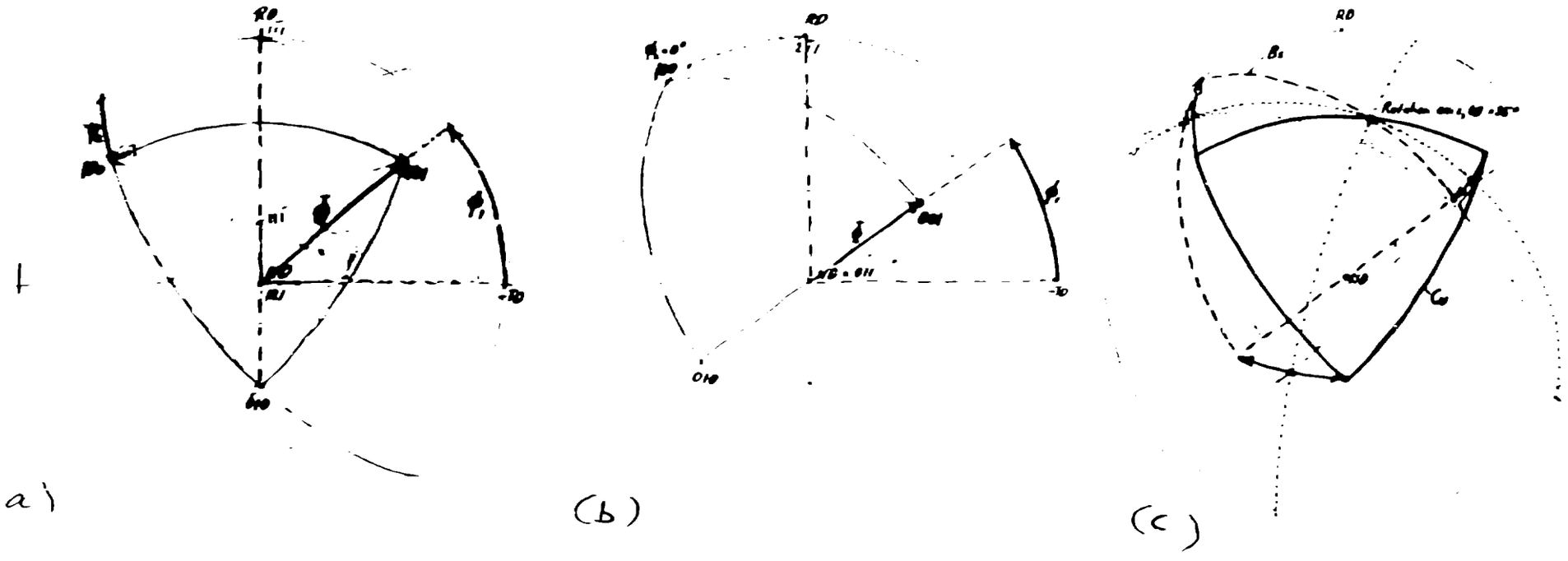

Fig. 10 Derivation of Orientation Relationships.
(a) Reconstruction of the crystal orientation for the maximum at $\phi_1 = 40°$, $\Phi = 66°$, $\phi_2 = 25°$ using the ODD of Fig. 9 and an equal-area net (Cu component).
(b) Same as (a) for the orientation $\phi_1 = 35°$, $\Phi = 45°$, $\phi_2 = 0°$ (B component).
(c) Superposition of (a) and (b) to determine the rotation axis and angle ω which brings the two orientations into coincidence.

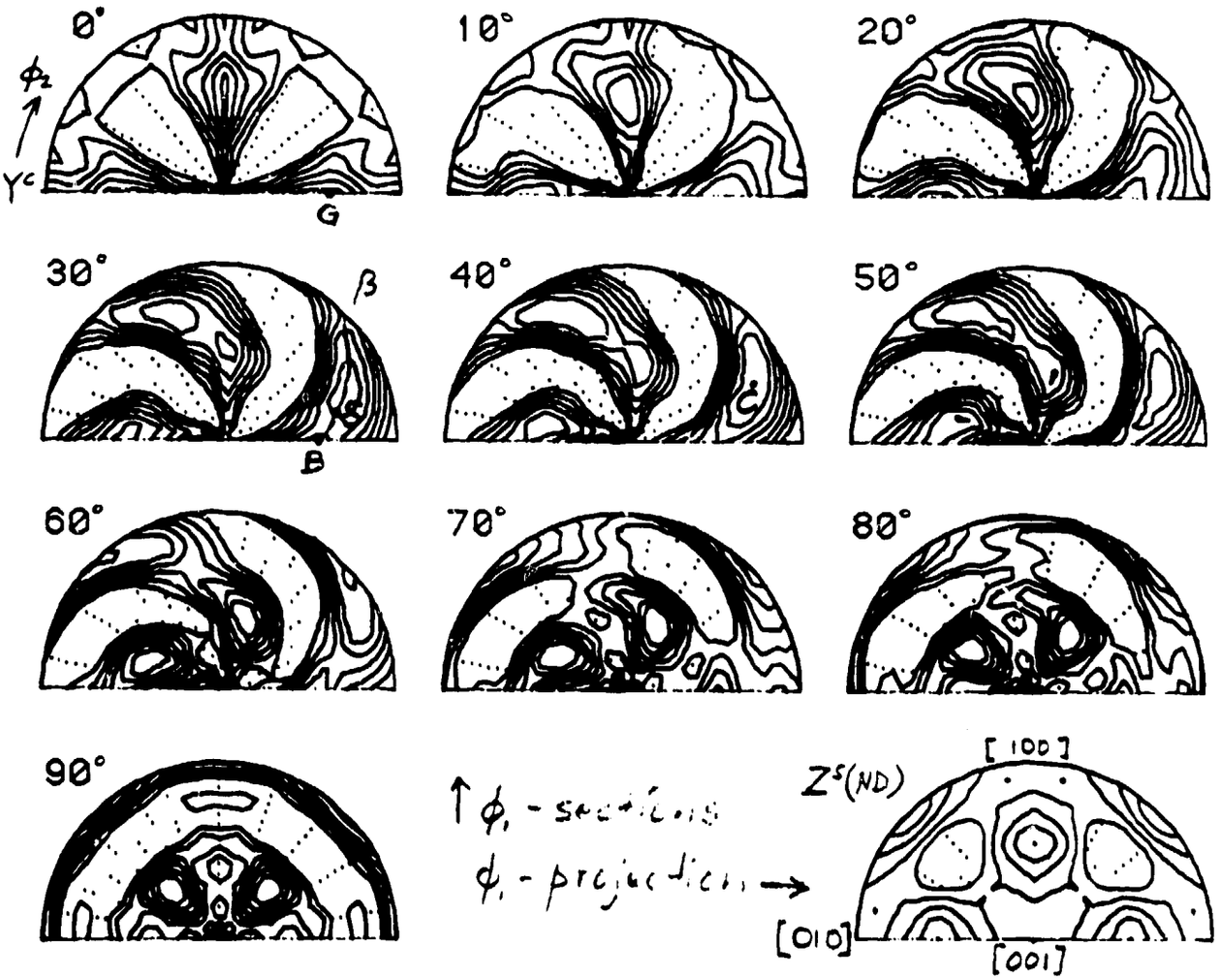

Fig. 11 SOD of rolled copper represented as partial inverse pole figures. The test diagram is an average over partial inverse pole figures from $\phi_1 = 0°$ to $\phi_1 = 180°$ and corresponds to an inverse pole figure for the ND axis (Fig. 5c). The letters indicate f.c.c. rolling components as in Fig. 9, and the 'β-fibre'.